Mechanical Behavior Analysis with the Finite Elements Method of Solar Collector's Tracking Systems

MIHAI TIBERIU LATES
Department of Product Design and Robotics
Transilvania University of Brasov
Eroilor street 29, 500068, Brasov
ROMANIA
latesmt@unitbv.ro http://www.unitbv.ro

Abstract: The paper presents the finite elements analysis of the mechanical behavior for three main solar collector tracking systems: for plate, for dish and for trough solar collectors; There are presented the modeling algorithm by using FEM, the characteristics of the loads and of the restrictions. Finally, the aim is to find out the critical position of the tracking systems, when the equivalent stresses and the displacements have a maximum value and to identify the free oscillations characteristics (modes, frequencies, accelerations). According to the conclusions can be compared, as mechanical behavior, the analyzed structure of the tracking systems.

Key-Words: Solar collector, Tracking system, FEM, Stresses, Displacements, Vibrations.

1 Introduction

The solar collectors are used to transform the energy from the sun in heat used for domestic heat water or for buildings heating [1, 2, 3]. According to their construction and functioning principles, the solar collectors are plate type, dish type and trough type.
The main components of a plate type solar collector are presented in the Figure 1 [4].

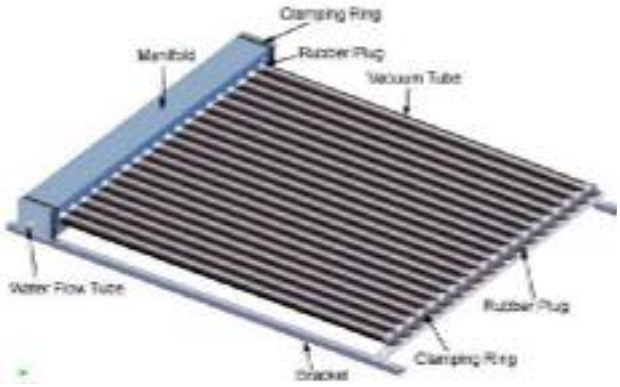

Fig.1

The dish type (Figure 2) [5] and trough type (Figure 3) [6] solar collectors are solar concentrator systems: the mirrors are disposed on a parabolic dish type or trough type surface and they orient the sun rays to an absorber pipe. The water inside the pipe is heated at high temperatures due to the action of the sun rays on a small surface.
The maximum amount of energy is collected from the sun when the solar collector's surface has a position normal to the solar radiation.

Fig.2

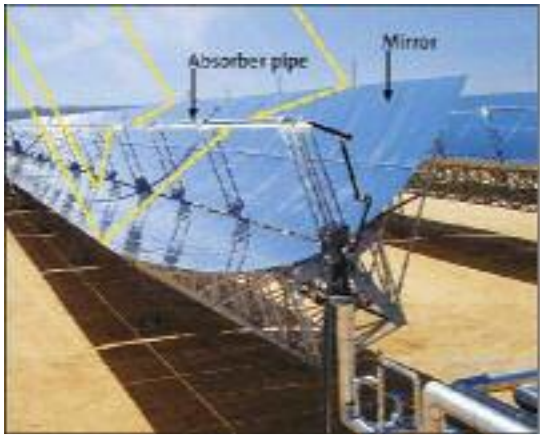

Fig.3

Figure 4 shows the normal orientation of the collector's surface to the sun rays (the horizontal plane represents the solar collector's surface) [7].

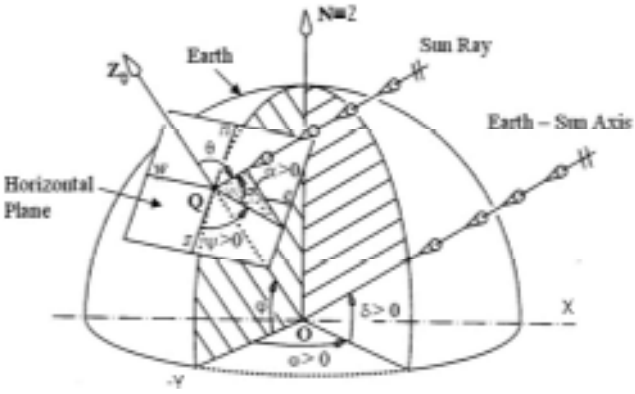

Fig.4

The global reference frame (attached to the Earth) is represented by the *OXYZ* reference frame. The position of the solar collector's surface is determined by the center point *Q* of the horizontal plane which indicates the North – South direction (the *n – s* line) and the West – East direction (the *w – e* line). The position of the Earth – Sun axis is given by the angle ω which represents the daily motion of the Earth and the angle δ which represents the seasonal motion of the Earth. For the *Q* point of the solar collector's surface the position is given by the angle ψ (for the daily motion) and the angle α (for the seasonal motion). The position of the point *Q* on the Earth's surface is given by the angle φ.
During the day-light time, as inverse relative motion, the sun has a diurnal motion from east to west. During one year the sun has a smaller seasonal motion from north to south. Due to these considerations, it is necessary to find solution on the way to orient the solar collectors surface normal to the solar radiation during a day light period and during one year, also. The solution is given by the tracking systems [1, 2, 3].

2 Problem Formulation

There are two types of tracking systems, mainly: tracking systems with one independent motion (according to the diurnal motion) and tracking systems with two independent motions (according to the diurnal and seasonal motions).
In the design process of the tracking system is important to find out the critical position of this, in order to identify the position when the equivalent stresses and the displacements values are maxim. The stresses and displacements fields are identified by using the finite elements method [8, 9, 10].

The modeling and analysis algorithm with the finite element method is presented in the Figure 5.
The modeling of the geometrical domain consists in the modeling of the component elements and than, by using specific constraints, the modeling of the assembly.

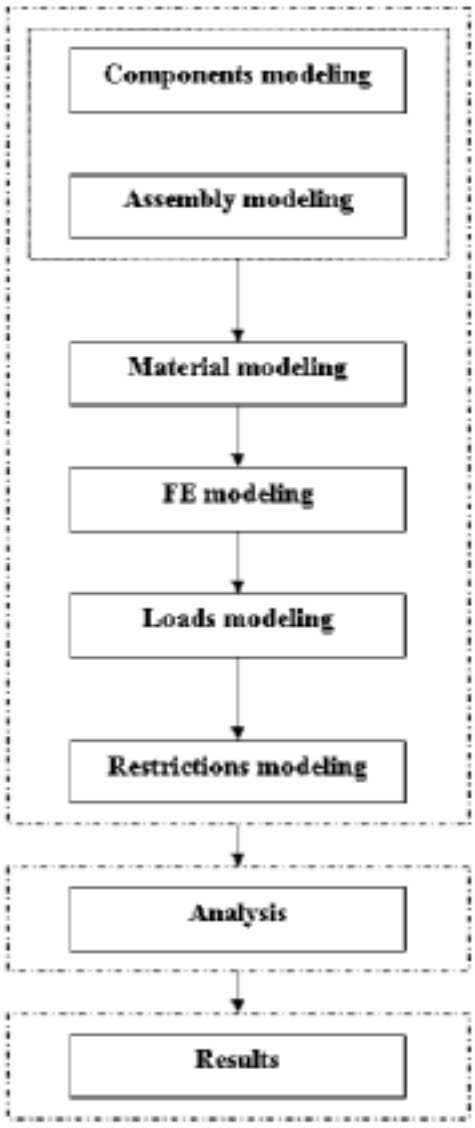

Fig.5

The material modeling is represented by the modeling of the mechanical properties for each material of the components (the *Young's* modulus, the *Poisson's* coefficient, the density).
The finite elements (FE) modeling consists in the process of choosing the type of the finite element (linear or parabolic, hexahedral or tetrahedral) and establishing of the size and of the maximum error from the real geometrical shape.
For the loads modeling the values and the type of the loads (concentrated or distributed forces, pressures, accelerations) are established.

The modeling of the restrictions is represented by the modeling of the connections (joints) between the component elements of the structure and the modeling of the connections (f. e. clamps) with the fixed parts (the ground).
The analysis is made by the software, automatically.
The results are presented as stresses and displacements fields, or as graphs.
Figure 6 … 8 show the finite element models of three main solar collector tracking systems with one independent motion: for plate, for dish and for trough solar collectors; the structures have the same width and the same cross-sectional area for the steel bars.

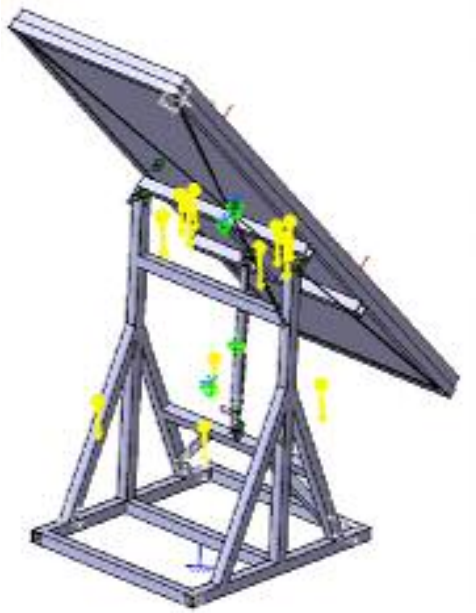

Fig.6

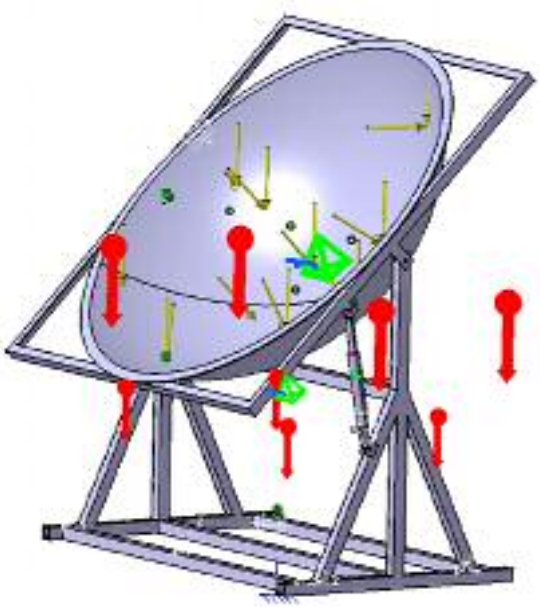

Fig.7

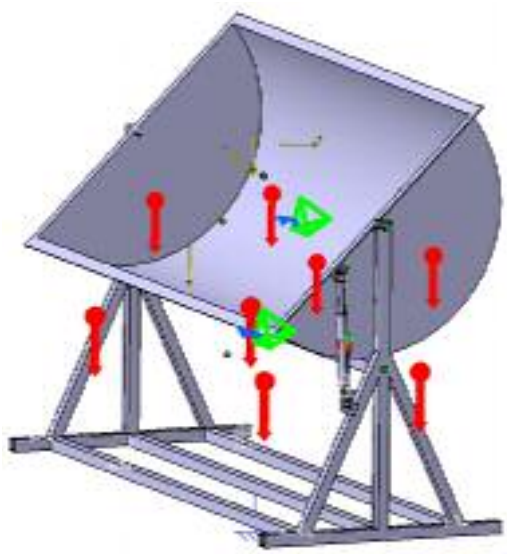

Fig.8

The materials characteristics, for each component of the tracking system, are defined as following [11, 12]:

- for the collector (made by glass): the *Young's* modulus $E= 6.5 \cdot 10^{10}$ N/m^2, the *Poisson's* coefficient $\nu=0.161$, the density $\rho=2190$ kg/m^3;
- for the collector's frame (made by aluminum): the *Young's* modulus $E= 7 \cdot 10^{10}$ N/m^2, the *Poisson's* coefficient $\nu=0.346$, the density $\rho=2710$ kg/m^3;
- for the tracing's components and the linear actuator (made by steel): the *Young's* modulus $E= 2 \cdot 10^{11}$ N/m^2, the *Poisson's* coefficient $\nu=0.266$, the density $\rho=7860$ kg/m^3.

The external loads are materialized by forces and pressures which are produced by extreme meteorological situations; it is considered a 30 cm thick snow layer on the collector's surface an a 16 m/s wind speed is acting on the structure (for higher wind speeds the collector is oriented in a horizontal position – according to the standards) [12, 13, 14, 15, 16, 17].
According to the collector's dimensions, the snow is acting with a weight force equal with 660 N on the collector's surface. For the static friction coefficient of the materials snow/glass, the snow is staying on the collector's surface until an inclination angle (from the vertical plane) equal with 21.71^o [17].
The modeling of the geometrical domain consists in the modeling of the component elements (the tracking system, the frame, the collector, the linear actuator); the final model results by assembling the component elements.

The constraints are represented by the clamp applied to the seating surface of the base and by the links between the component elements [12, 13, 14, 15, 17].
The finite elements analysis is done by considering the orientation angle between [-45^0, 45^o]; the 0^o value for the angle is considered when the solar collector's frame is parallel to the ground.
The analysis of the vibration frequencies and shapes is useful to avoid the resonance phenomenon due to the action of the external dynamic loads, as wind or earthquake.
The general numerical model of the structure, achieved with the finite element method is represented by the equation [14]

$$[M]\left[\ddot{D}\right]+[C]\left[\dot{D}\right]+[K][D]=[Q], \quad (1)$$

where: $[Q]$ represents the nodal loads matrix; $[M]$ – the mass matrix (contains the masses of each component); $[D]$ – the nodal displacements matrix; $\left[\dot{D}\right]$ – the nodal velocities matrix; $\left[\ddot{D}\right]$ – the nodal accelerations matrix; $[C]$ – the structure's damping matrix; $[K]$ – the structure's stiffness matrix.
In the case of the free frequencies (without the action of the loads) the numerical model is

$$[M]\left[\ddot{D}\right]+[C]\left[\dot{D}\right]+[K][D]=[0]. \quad (2)$$

Without damping, the oscillations (vibrations) of the structure are producing, theoretically to the infinite, until the period when the structure is damaged (the oscillations amplitude is constant in time). In this case the numerical model is

$$[M]\left[\ddot{D}\right]+[K][D]=[0]. \quad (3)$$

The oscillations frequencies are the free frequencies instead; the equation of the oscillations is

$$[D]=\left[\overline{D}\right](\cos\omega t+i\sin\omega t) \quad (4)$$

where $\omega=2\pi\nu$ is the pulsation of the oscillations with the frequency ν and $\left[\overline{D}\right]$ is the matrix of the oscillations amplitude.
So, the relation (3) will be

$$\left([K]-\omega^2[M]\right)\left[\overline{D}\right]=[0]. \quad (5)$$

To find the solutions of the equation (5) is necessary to solve the equation

$$\left|[K]-\omega^2[M]\right|=0. \quad (6)$$

By solving the equation (6) the natural pulsations ω_i and the natural frequencies ν_i will be established.

3 Problem Solution

The following figures are presenting the stresses and displacements fields for plate, dish and trough type solar collectors, respectively [17].
The stresses and displacements fields are shown for the orientation position of 45^o. In this case the stroke of the linear actuator has a minimum value and the stresses and displacements maximum values are maximum.

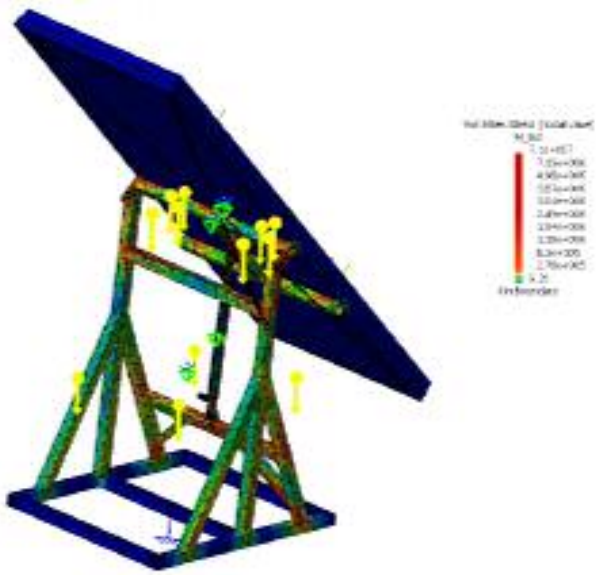

Fig.9

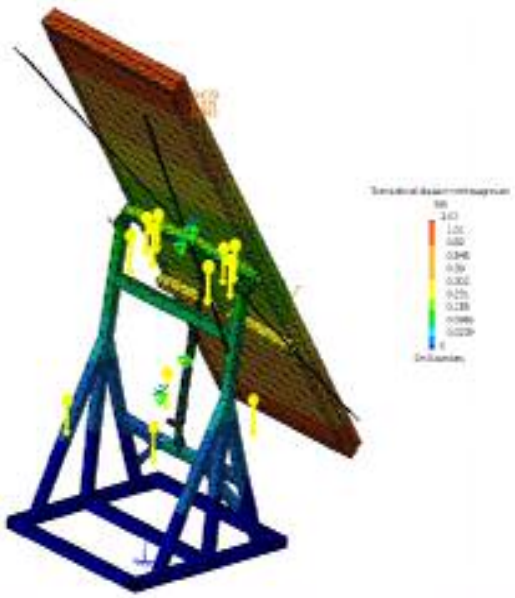

Fig.10

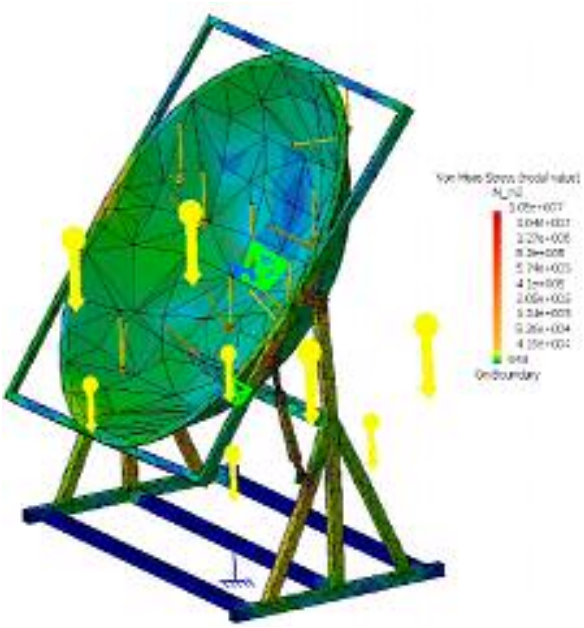

Fig.11

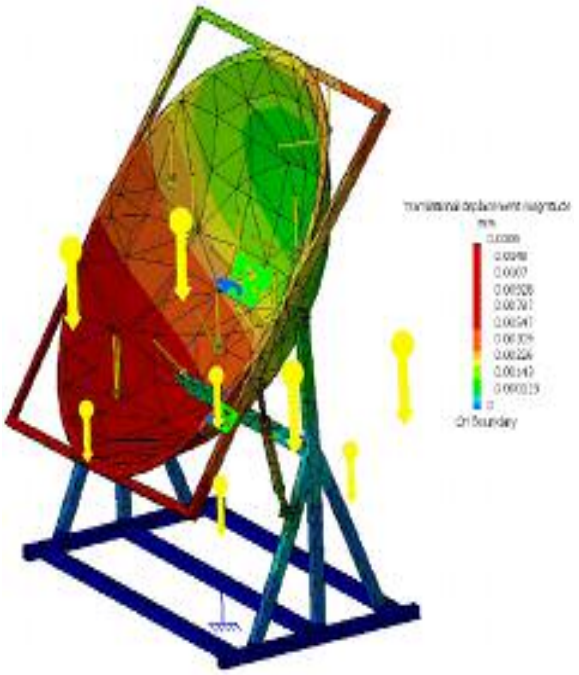

Fig.12

On the presented figures it can be observed that the equivalent stresses are having maximum values in the rotational joints between the supporting frames, the basic structures and the linear actuators. The values of the maximum equivalent stresses are: 71 MPa for the plate solar collector; 10.5 MPa for the dish type solar collector; 34.4 MPa for the trough type solar collector. The displacements have small values (less than 1.02 mm).

The variation of the maximum equivalent stresses and of the maximum displacements, for the plate, dish and trough type solar collectors with the orientation angle is presented in figures 15 … 20 [17].

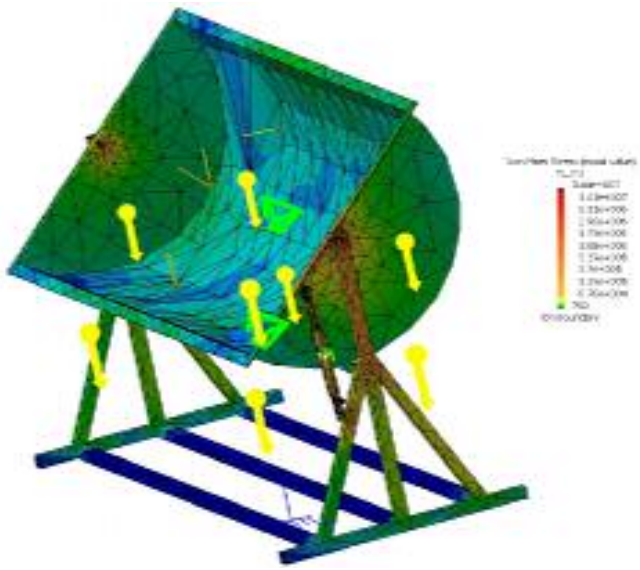

Fig.13

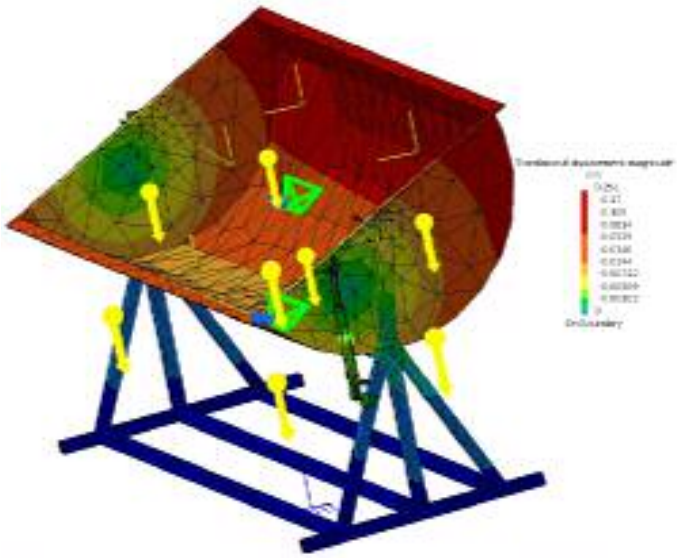

Fig.14

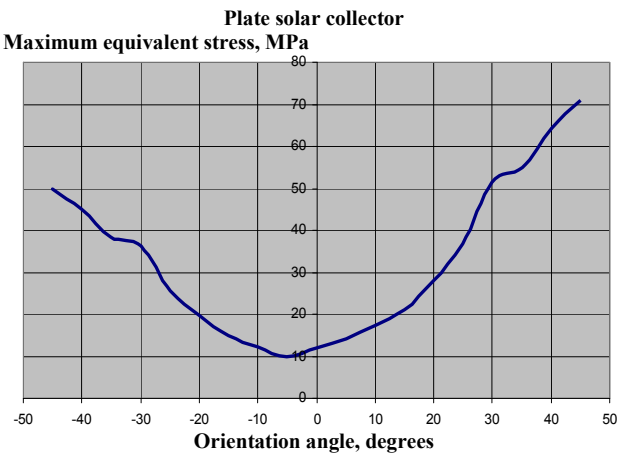

Fig.15

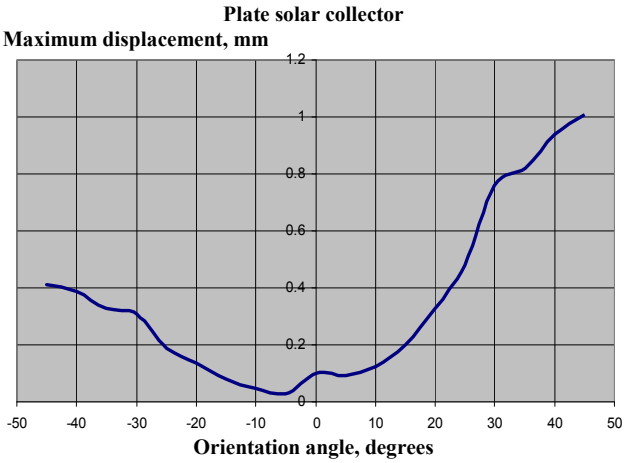

Fig.16

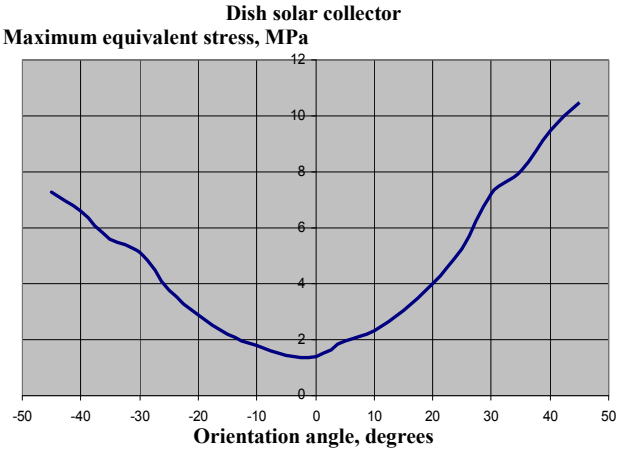

Fig.17

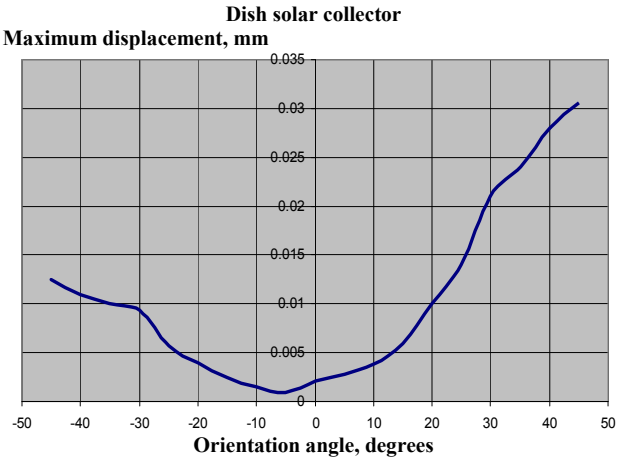

Fig.18

In the case of maximum values for the equivalent stresses and displacements, the analysis of the oscillations frequencies and modes is achieved. Figure 21, 22 and 23 are presenting the 10 vibration modes for the plate, dish and trough type solar collectors tracking systems, respectively. The values of the frequencies are presented in the figures 24, 25 and 26, respectively.

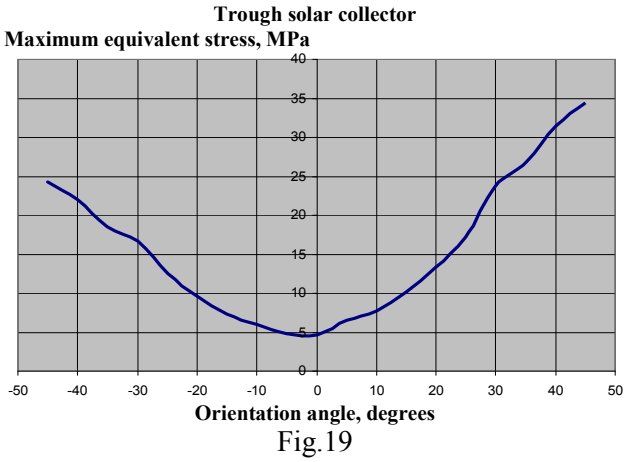

Fig.19

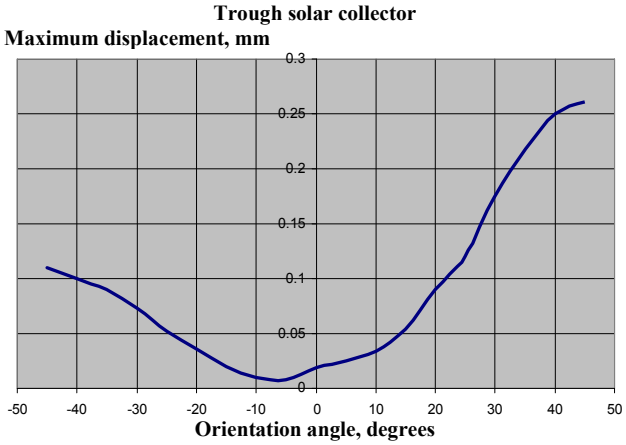

Fig.20

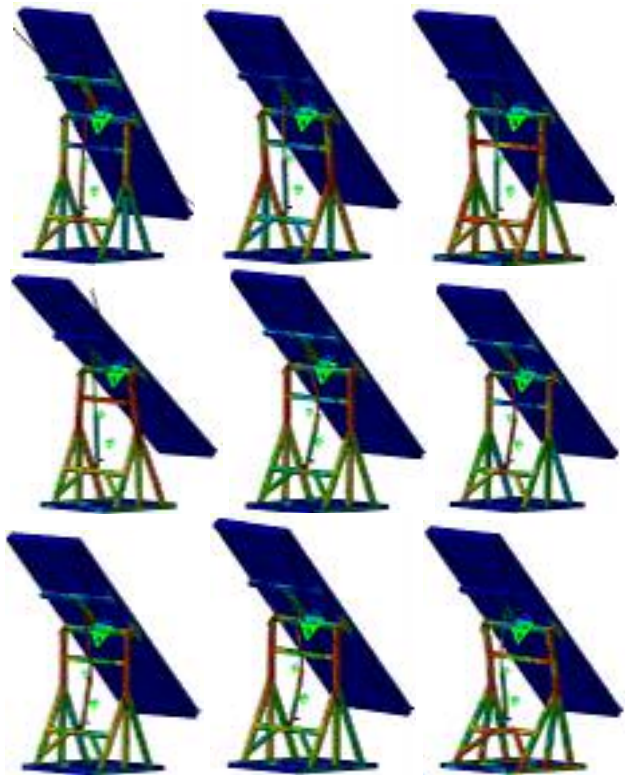

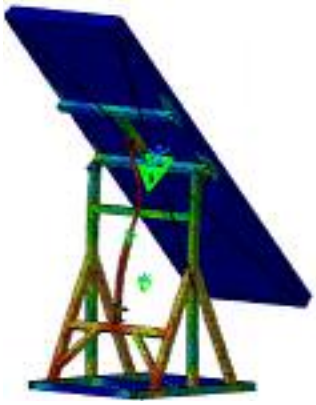

Fig.21

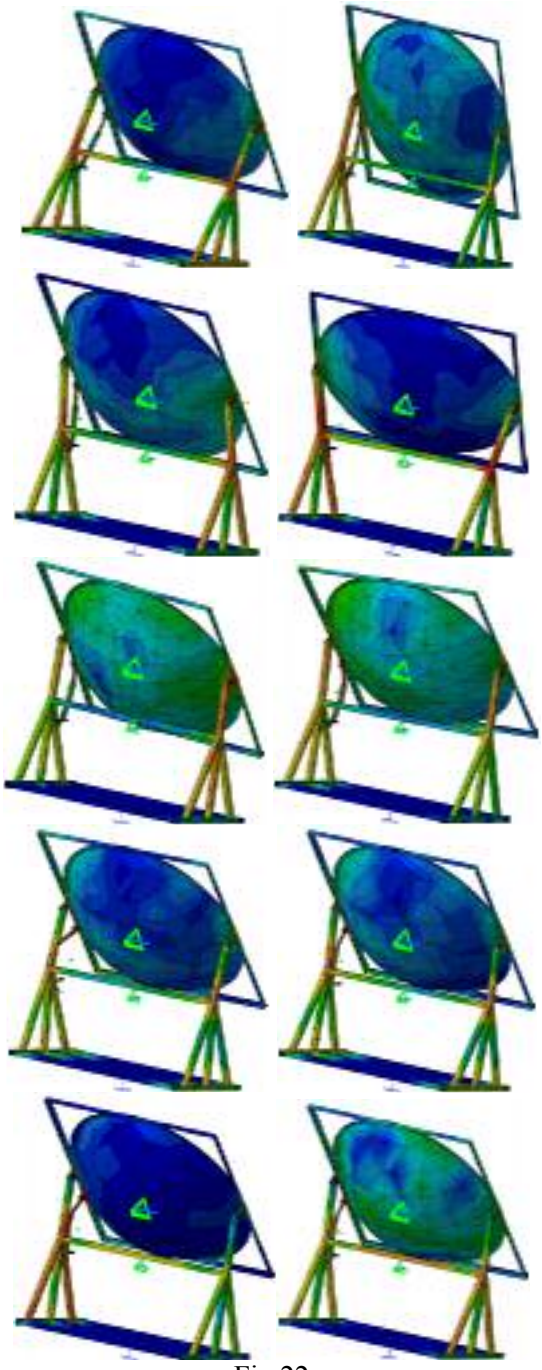

Fig.22

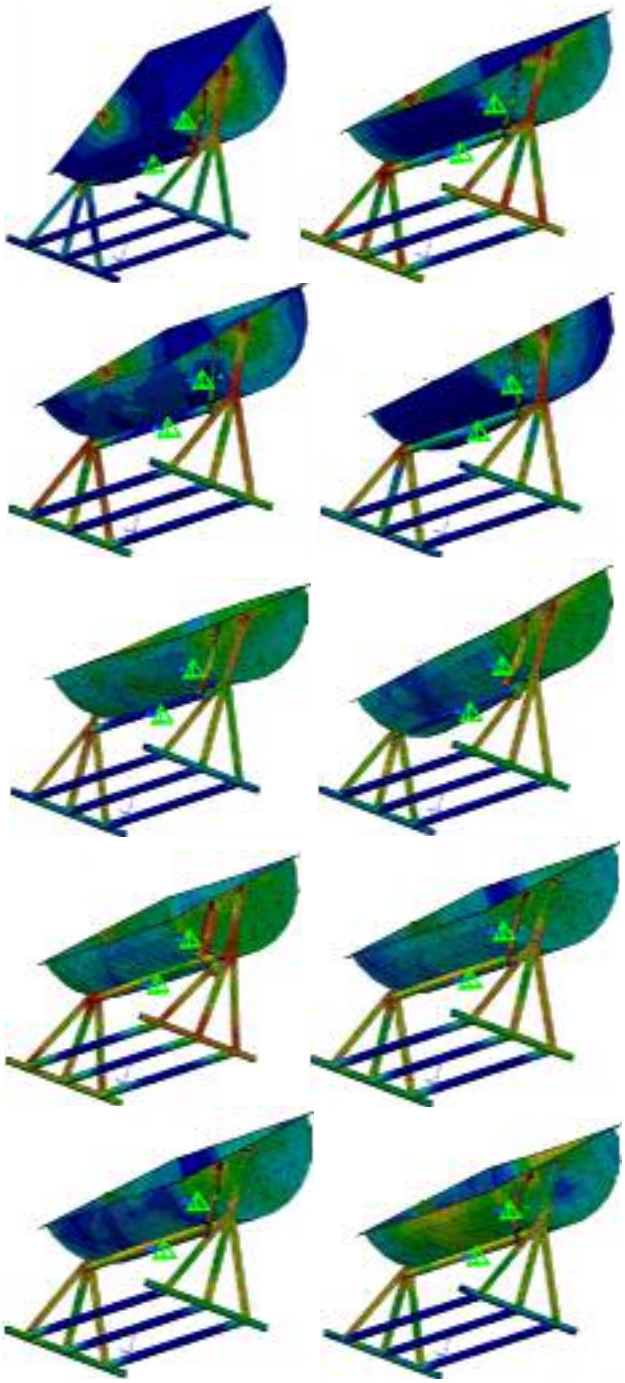

Fig.23

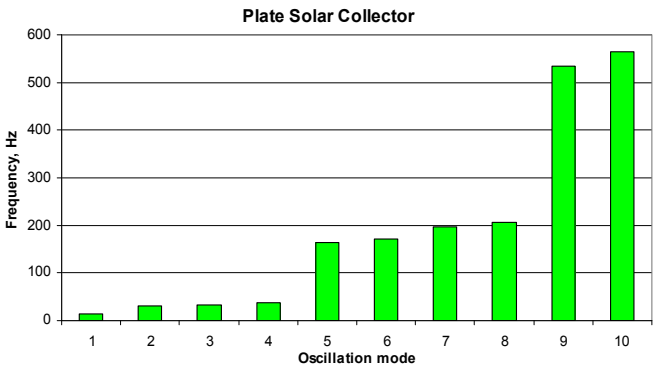

Fig.24

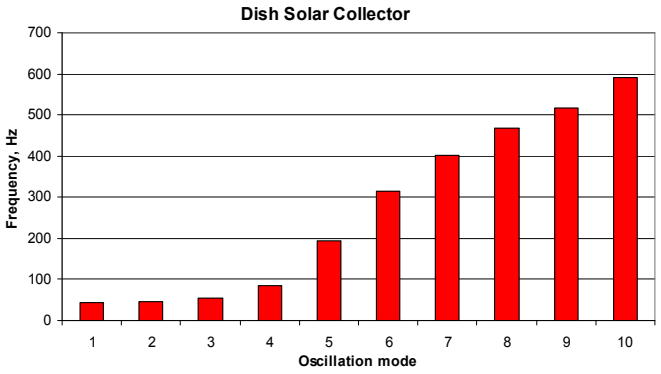

Fig.25

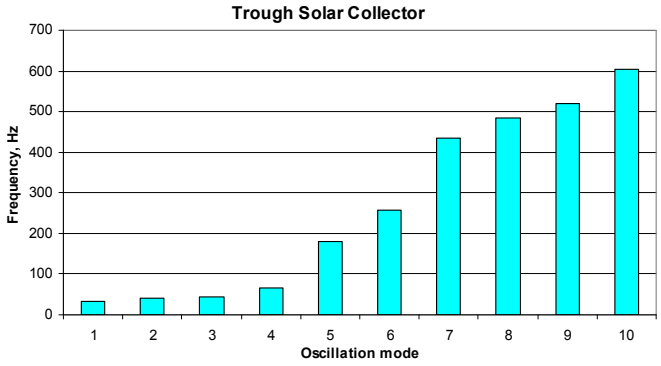

Fig.26

The values of the free frequencies are important in the order to avoid the resonance phenomenon (f. e. these values should be different from the earthquakes frequencies values in the location where the solar collectors tracking systems are implemented).

Oscillation of the plate type solar collector

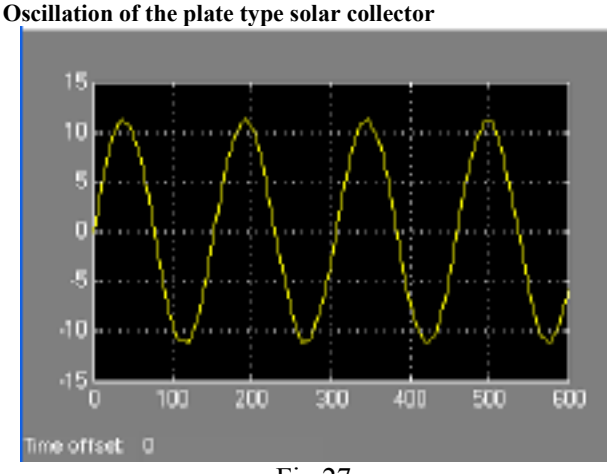

Fig.27

In the case of free oscillations the shape of the oscillations of each structures (the tracking system of the plate type, of the dish type and of the trough type solar collector) is presented in the Figures 27, 28 and 29 respectively. The simulation was achieved, according to the equation (4), by considering for each structure, the characteristics (frequency and amplitude, in mm) of the first mode of vibration for a simulation time of 10 min.

High values for the oscillations amplitudes are obtained for the plate type solar collector tracking system (11.3 mm). The biggest value of the oscillations frequency is obtained for the dish type solar collector tracking system (42.3964 Hz).

Oscillation of the dish type solar collector

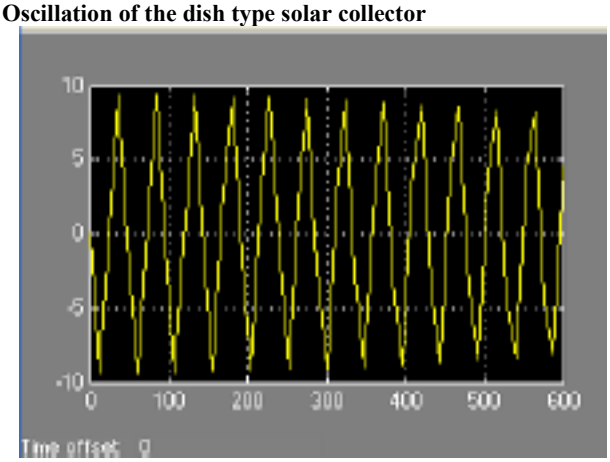

Fig.28

Oscillation of the trough type solar collector

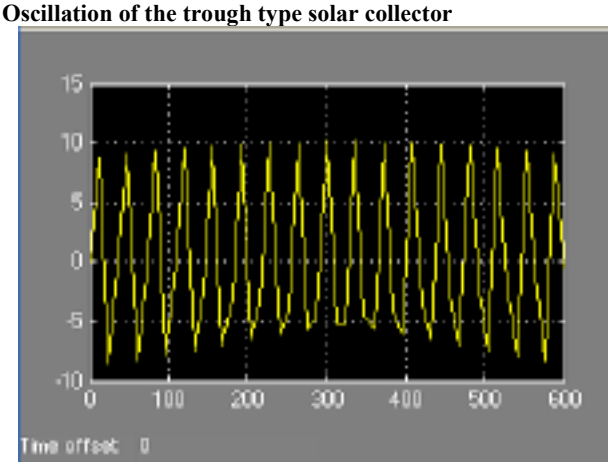

Fig.29

Oscillations acceleration of the plate type solar collector

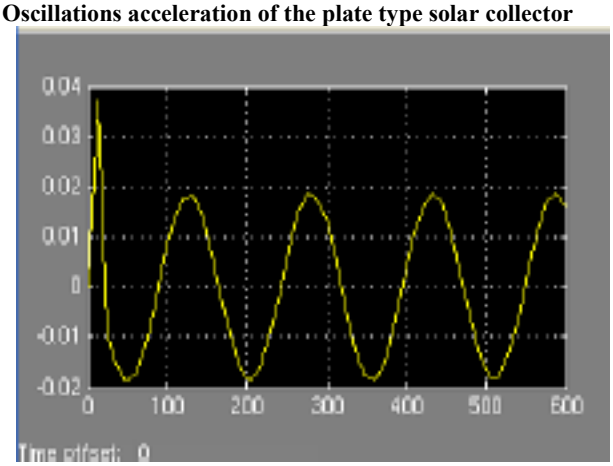

Fig.30

The mechanical behavior is influenced by the acceleration of the oscillations. Figure 30, 31 and 32 present the evolution for the accelerations of the oscillations for the plate type, dish type and of the trough type solar collectors tracking systems.

Oscillations acceleration of the dish type solar collector

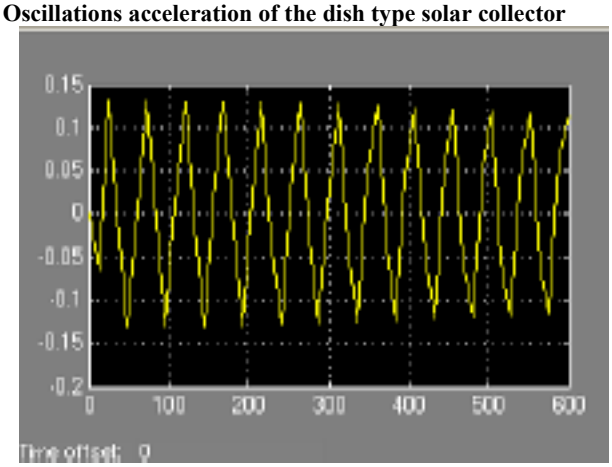

Fig.31

Oscillations acceleration of the trough type solar collector

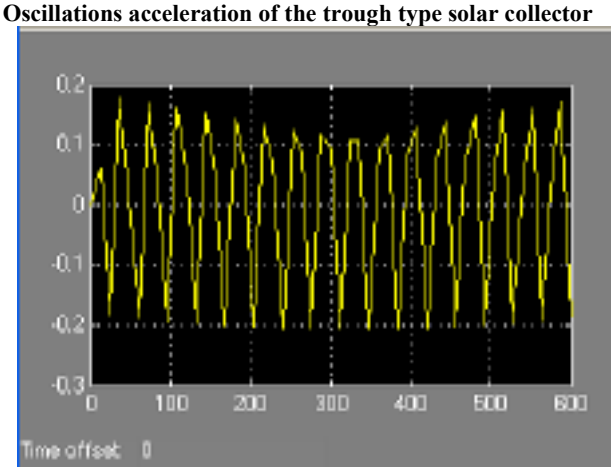

Fig.32

According to the graphs the plate type solar collector tracking system has small shocks of oscillation (the acceleration is 0.02 mm/s – 0.04 in the transitory period). The biggest shocks are in the case of the trough type solar collector tracking system (the acceleration value is 0.2 mm/s).

4 Conclusion

According to the results obtained form the finite elements analysis of the presented solar collectors tracking systems, some important conclusions can be issued [17]:

- the maximum values of the equivalent stresses are obtained in the rotational joints of the structures (the joints between the frame, supporting structure and the linear actuator);
- the maximum values of the equivalents stresses are the following: 71 MPa for the plate type solar collector, 10.5 MPa for the dish type solar collector and 34.4 MPa for the trough type solar collector;
- to reduce the maximum stresses there are imposed new constructive solutions for the rotational joints (bigger bolts);
- the maximum values of the displacements are small (the maximum value of the displacement is obtained in the case of plate type solar collector – 1.02 mm) and the influence on functioning of the tracking system is insignificant;
- the maximum values of the equivalent stresses and displacements are obtained for big orientation angles (in this case the actuator stroke has a minimum stroke and it means that the structure is a stabile one);
- the cause of the different values for the stresses and displacements is the overall dimension of the three solar collectors (so, the mass) which determine the footprint of the sustaining structure. In future design, to improve the values of the stresses and displacements, higher cross-sectional areas for the steel bars could be used;
- according to the simulations achieved for the first mode of vibration, high values for the oscillations amplitudes are obtained for the plate type solar collector tracking system (11.3 mm).
- the biggest value of the oscillations frequency is obtained for the dish type solar collector tracking system (42.3964 Hz);
- the values of the free frequencies are important in the order to avoid the resonance phenomenon (f. e. these values should be different from the earthquakes frequencies values in the location where the solar collectors tracking systems are implemented);
- the plate type solar collector tracking system has small shocks of oscillation (the acceleration is 0.02 mm/s – 0.04 in the transitory period).

References:

[1] J. A. Duffie a. o., *Solar Engineering of Thermal Processes*, John Wiley & Sons Inc., USA, 1991.

[2] R. Lates, I. Vişa, Solar Collectors – An Overview, *Proceedings of Conference of*

Sustainable Energy, Brasov, Romania, 7-9 July 2005.

[3] R. Lates, I. Vişa, C. Lăpuşan, Mathematical Optimization of Solar Thermal Collectors efficiency Function Using MATLAB, *Proceedings of The 4th IASME / WSEAS International Conference on Energy, Environment, Ecosystems and Sustainable Development (EEESD'08)*, University of Algarve, Faro, Portugal, 11 – 13 June 2008. pp.42-46.

[4] www.made-in-china.com

[5] www.solarmillennium.de

[6] www.infinilec.com

[7] I. Vişa a. o., On the Dependence BETWEEN THE Step Orientation and the Received Direct Solar Radiation of a PV Panel, *CD Proceedings of The International Conference on Renewable Energy and Power Quality*, Santander, Spain, 2008.

[8] P. K. Barnerjee, *The Boundary Element Methods in Engineering*, Mc Graw-Hill Publishing House, Maidenhead, England, 1993.

[9] G. Bee, J. O. Watson, *Introduction to Finite and Boundary Element Methods for Engineers*, John Wiley & Sons Publishing House, Chichester, England, 1992.

[10] M. Gerardin, A. Cardona, *A. Flexible Multibody Dynamics: A Finite Element Approach*, John Wiley & Sons Publishing House, Chichester, England, 2001.

[11] M. J. Fagan, *Finite Element Analysis. Theory and Practice*, Longman Group, England, 1992.

[12] O. C. Zienkiewicz, R. L. Taylor, *The Finite Elements Method*, Vol. II. Mc Graw-Hill Publishing House, Maidenhead, England, 1989.

[13] M. T. Lates, *Metoda Elementelor Finite în Inginerie. Aplicatii*, Editura Universitatii Transilvania din Brasov, Romania, 2008.

[14] G. L. Mogan, *Metoda Elementelor Finite in Inginerie. Bazele Teoretice*, Editura Lux Libris, Brasov, Romania, 1997.

[15] O. C. Zienkiewicz, R. L. Taylor, *The Finite Elements Method*, Vol. I. Mc Graw-Hill Publishing House, Maidenhead, England, 2006.

[16] C. I. Cosoiu, A. Damian, R. M. Damian, M. Degeratu, Numerical and Experimental Investigation of Wind Induced Pressures on a Photovoltaic Solar Panel, *Proceedings of The 4th IASME / WSEAS International Conference on Energy, Environment, Ecosystems and Sustainable Development (EEESD'08)*, University of Algarve, Faro, Portugal, 11 – 13 June 2008. pp.74-80.

[17] M. T. Lates, R. S. Lates, Analysis with the Finite Elements Method of Solar Collector's Tracking System, *Proceedings of The 4th IASME / WSEAS International Conference on Energy, Environment, Ecosystems and Sustainable Development (EEESD'08)*, University of Algarve, Faro, Portugal, 11 – 13 June 2008. pp.42-46.